Hydrogenation induced reversible modulation of perpendicular magnetic coercivity in Pd/Co/Pd films

Wen-Chin Lin, Cheng-Jui Tsai, Bo-Yao Wang, Chao-Hung Kao, and Way-Faung Pong

Articles you may be interested in

Critical hydrogenation effect on magnetic coercivity of perpendicularly magnetized Co/Pd multilayer nanostructures
J. Appl. Phys. **116**, 073904 (2014); 10.1063/1.4893588

Time-dependent magnetization reversal in amorphous CoSiB/Pd multilayers with perpendicular magnetic anisotropy
J. Appl. Phys. **113**, 17A342 (2013); 10.1063/1.4801425

Two different coercivity lattices in Co/Pd multilayers generated by single-pulse direct laser interference lithography
J. Appl. Phys. **105**, 113915 (2009); 10.1063/1.3126714

Quantitative correlation between the local coercivity variation and magnetization reversal dynamics in Co/Pd multilayer thin films
J. Appl. Phys. **93**, 10143 (2003); 10.1063/1.1577220

In situ vectorial magnetization reversal study of ultrathin Co films on Pd (111) using magneto-optical Kerr effects
Appl. Phys. Lett. **81**, 91 (2002); 10.1063/1.1490632

Hydrogenation induced reversible modulation of perpendicular magnetic coercivity in Pd/Co/Pd films

Wen-Chin Lin,[1,a)] Cheng-Jui Tsai,[1] Bo-Yao Wang,[2] Chao-Hung Kao,[2] and Way-Faung Pong[2]

[1]Department of Physics, National Taiwan Normal University, Taipei 116, Taiwan
[2]Department of Physics, Tamkang University, Tamsui 251, Taiwan

In perpendicularly magnetized Pd/Co/Pd trilayers, the hydrogenation not only increased Kerr signal but also significantly enhanced the magnetic coercivity (H_C) by 17%. The reversibility was demonstrated by cyclic H_2 exposure. The time constants of hydrogen absorption and desorption effect on H_C range from tens to hundreds seconds, depending on the H_2 gas pressure. The magneto-optical Kerr signal and magnetic coercivity was simultaneously recorded during H_2 absorption and desorption. These multifarious signals respond differently and provide a detailed understanding of hydrogenation effect on the functional Pd/Co/Pd trilayers. © 2013 AIP Publishing LLC.
[http://dx.doi.org/10.1063/1.4812664]

Metal-hydride systems have been widely studied in the last decades due to the potential of hydrogen storage and sensing. Hydrogen is able to modify the crystalline structure, morphology, and especially the electronic structures; meanwhile, the optical and magnetic properties are modulated.[1,2] Based on this idea, hydrogenated metallic films are considered as functional materials in high tech application.[2] Pd is usually used as a catalyst for hydrogen dissociation and absorption.[2–6] In the initial stage, H atoms occupy the interstitial sites of the Pd crystalline lattice (α phase). With increasing hydrogen absorption, the Pd lattice is expanded by 2–3% (β phase).[7–9] Therefore, Pd thin films of few nm thickness are widely used in metal-hydride systems.[10] Many studies have been devoted to the combination of Pd layers with other functional thin films for the investigation of hydrogenation effect.[7,11,12] The hydrogenation of Pd capping layer may induce proximity effect upon the underneath functional thin films. This effect is important from fundamental point of view and also applicable in future techniques. Especially, some studies have focused on the combination of hydride-metal with magnetic materials. For example, long range magnetic interlayer coupling in Fe/V and Fe/Nb multilayers change signs, because hydrogen adsorption changes the electronic structures of V and Nb intermediate layers.[13–15] Recently, Chang et al. reported on using the metallic spintronic thin film as a hydrogen sensor.[16] Lederman et al. reported on 50% magneto-optical (MO) enhancement in a hydrogenated Pd/Fe bilayer sample.[5] Our previous studies also investigated the reversible MO enhancement with the variation of Pd thickness and different magnetic underlayers.[17,18] However, in all of these Pd/Fe, Co, and Ni bilayers, only the MO enhancement was observed. The intrinsic magnetic behavior, like magnetic coercivity and magnetic anisotropy, was invariant with hydrogenation. In magnetism, Pd is also a particular element for the promotion of perpendicular magnetic anisotropy, which is a key issue in magnetic storage and sensor.[19,20] Pd/Co/Pd trilayers were used in this study. Post-annealing promoted the alloy formation at the Pd/Co interface and led to the enhanced surface magnetic anisotropy, which dominated the perpendicular magnetization.[20] The hydrogenation effect on perpendicularly magnetized Pd/Co/Pd thus is an interesting system to explore. Okamoto et al. first reported on the reduction of magnetization and the enhancement of magnetic anisotropy in hydrogenated Pd/Co/Pd trilayers with hydrogen gas pressure from 1.3 atm to 3 atm.[21] The hydrogen absorption in Pd/Co/Pd caused irreversible enhancement of Pd(111) orientation along with the significant increase in perpendicular magnetic anisotropy. After dehydrogenation, the magnetic anisotropy did not recover the initial value of un-hydrogenated state. In 2011, K. Munbodh et al. reported another experiment of Pd/Co/Pd using polarized neutron reflectivity.[7,22] The observed hydrogen effects on magnetization and magnetic anisotropy were similar to the results of Okamoto et al. However, until now, no well reversible control of magnetic anisotropy was achieved through hydrogenation. The detailed studies of response time and the sensitivity to the different hydrogen gas pressure are still lacking. Thus, in this experiment, we thoroughly investigate the reversible hydrogenation effect on perpendicular magnetic anisotropy of Pd/Co/Pd trilayers using the hydrogen gas pressure from 10 to 1000 mbar. The optical, magneto-optical, and magnetic properties were simultaneously recorded for the understanding of the detailed mechanism in hydrogenation and dehydrogenation.

The 5 nm Pd/4 nm Co/5 nm Pd thin trilayers were deposited on Al_2O_3(0001) substrate by e-beam heated evaporators in an ultra-high vacuum (UHV) chamber with a base pressure of 3×10^{-9} torr.[17] Post-annealing at 700 K was in situ carried out right after deposition. The magnetic properties were investigated at room temperature (RT) using magneto-optical Kerr effect (MOKE). The MOKE measurement system was composed of four electromagnet poles installed in a vacuum chamber. The MOKE hysteresis loops were measured in both perpendicular and in-plane geometry by simply switching the polarity of electromagnet without changing the optical setup. The MOKE chamber was either in air or pumped to a vacuum of 5×10^{-2} Torr. Afterward the MOKE chamber was filled

a)E-mail: wclin@ntnu.edu.tw

with different hydrogen pressure in order to investigate the hydrogenation-induced effect on the magneto-optical and magnetic properties.

Fig. 1(a) shows the in-plane MOKE hysteresis loops of the as-deposited (non-annealed) Pd/Co/Pd measured in air, vacuum, and 1 atm hydrogen gas pressure. The as-deposited Pd/Co/Pd trilayers on $Al_2O_3(0001)$ exhibited only in-plane magnetism. The Kerr signal is clearly enhanced, but the magnetic coercivity (H_C) is always invariant, like our previous
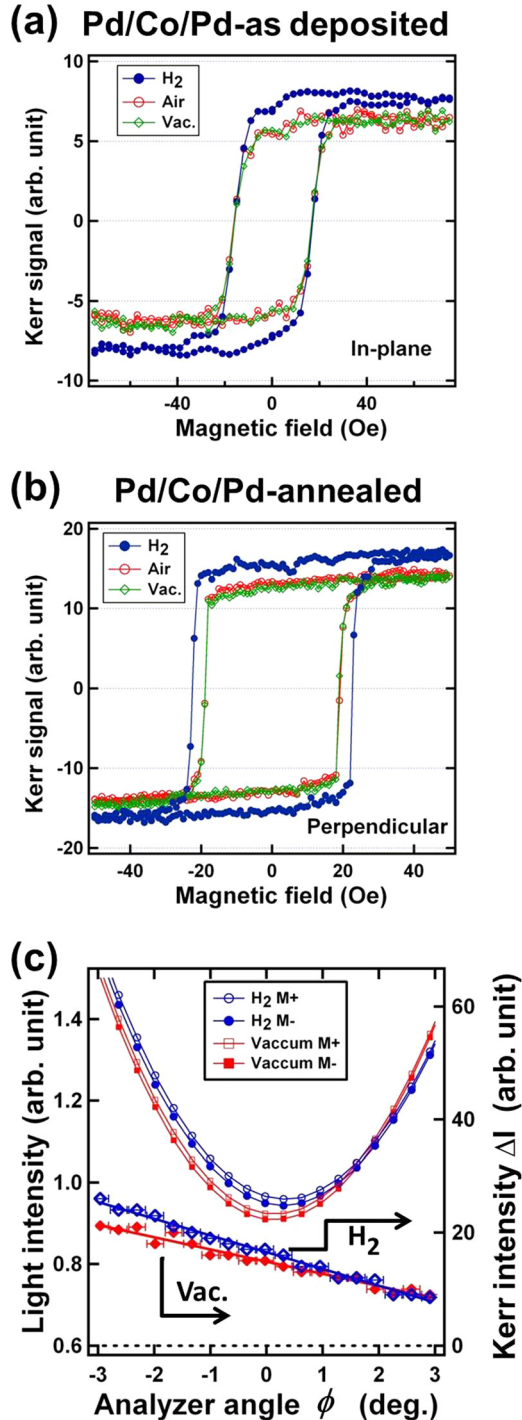
(a) Pd/Co/Pd-as deposited

(b) Pd/Co/Pd-annealed

(c)

FIG. 1. MOKE hysteresis loops measured in air, vacuum, and 1 atm H_2 gas for (a) as-deposited and (b) post-annealed 5 nm Pd/4 nm Co/5 nm Pd tri-layers. (c) Light intensity $I_{\pm m}$ (upper part, left axis) and Kerr intensity $\Delta I = I_{+m} - I_{-m}$ (lower part, right axis) measured in vacuum and 1 atm H_2 gas, respectively.

studies on Pd/Fe, Co, Ni bilayers.[17,18] This indicates H_2 adsorption does not affect the magnetization processes of magnetic films, and the MO enhancement should originate from H_2-induced change of Pd optical properties.[10,17,18,23–25] On the other hand, the post-annealed Pd/Co/Pd preferred an oblique magnetic easy axis. Magnetic hysteresis loops of comparable H_C were observable in both perpendicular and in-plane MOKE geometry. Fig. 1(b) shows the perpendicular MOKE hysteresis loops of the post-annealed Pd/Co/Pd measured in air, vacuum, and 1 atm hydrogen gas pressure. After exposure to 1 atm hydrogen gas, not only the magneto-optical Kerr signal but also the magnetic coercivity H_C was increased. The samples of Figs. 1(a) and 1(b) were grown with the same conditions. The only difference is the post-annealing treatment. Post-annealing promoted the alloy formation at Co/Pd interface, which resulted in the perpendicular anisotropy. The interface properties of the Pd/Co/Pd films were also characterized via surface sensitive Co L-edge X-ray absorption near edge structure (XANES) in total energy yield (TEY) mode, in which the XANES signal is known to be exponentially damped with increasing distance of elements away from the surface. Our measurements show that the intensity of Co L-edge XANES significantly increased for the Pd/Co/Pd films after annealing at 700 K. The non-annealed film showed only about 1/10 intensity of Co L-edge XANES as compared with the annealed film. Since both films were prepared in identical condition, the significant enhancement of Co XANES signal can be attributed to a diffusion of Co atoms from middle Co layer into the top Pd layer. Intuitively the significant contrast of H_C enhancement between the post-annealed and non-annealed Pd/Co/Pd might result from the hydrogenation of the Pd/Co alloy interface, since the interface anisotropy dominated the magnetic behavior. Because hydrogen absorption has been reported to change the electronic structure of Pd significantly, the hydrogen-induced modulation of magnetic coercivity observed in Fig. 1(b) could be due to the fact that hydrogen changes the spin-orbit coupling of Pd, especially at the Pd-Co alloy interface.

In our MOKE measurement, a *p*-polarized 670 nm laser was shone on the sample with an incident angle of 45°. The reflected beam was detected by an analyzer, which was composed of a linear polarizer at a small angle ϕ from the *s*-axis and a photodiode. When the sample is magnetic, the reflected beam is no more purely *p*-polarized. Instead, it is composed of a *p*-component (E_p) and an *s*-component (E_s).[26] The ratio of E_s / E_p is expressed as $\theta + i\epsilon$, where θ is the Kerr rotation, and ϵ is the Kerr ellipticity. When ϕ is very small, the measured light intensity I can be expressed as a parabolic function of ϕ, like Eq. (1) and the data curves in Fig. 1(c).[17,26]

$$I_{\pm m} = |E_p|^2 (\phi^2 + 2\theta_{\pm m}\phi + \theta_{\pm m}{}^2 + \epsilon_{\pm m}{}^2). \qquad (1)$$

The indexes of $\pm$m indicate the values corresponding to the positively/negatively magnetization state. The saturation Kerr rotation, defined as $\Delta\theta = (\theta_{+m} - \theta_{-m})/2$, is obtained from the shift of the extinction (minimum) angle of the two parabolas of the positively and negatively magnetized sample, i.e., $\pm$m. When the magnetization is switched, the change of intensity $\Delta I = I_{+m} - I_{-m}$, named Kerr intensity, is a linear function of analyzer angle ϕ, as shown in

Eq. (2).[17,26] The slope of Kerr intensity ΔI is proportional to $|E_p|^2$ and $\Delta\theta$. The lower panel of Fig. 1(c) shows the Kerr intensity ΔI deduced from the difference between experimental curves of the parabolic functions $I_{\pm m}(\phi)$.[17] The solid lines are obtained by the linear fitting. The reflectivity $|E_p|^2$ and the saturation Kerr rotation $\Delta\theta$ are deduced from fitting the parabolic curves $I_{\pm m}(\phi)$ and the linear functions $\Delta I(\phi)$ in Fig. 1(c).[17] $|E_p|^2$ determines the curvature of parabolic function and corresponds to the reflectivity of sample, especially the top layer of Pd. According to our fitting results, the reflectivity $|E_p|^2$ is decreased by 7% after hydrogen exposure. This is consistent with previous studies. Matelon *et al.* reported the hydrogenation-induced reduction of reflectivity reached 8% for 7.6 nm Pd/Si(111) and 16% for 7.6 nm Pd/Al$_2$O$_3$(110).[10] Besides, our fitting also shows that after hydrogenation, the saturation Kerr rotation $\Delta\theta$ is significantly enhanced by 45%, from 9×10^{-3} to 13×10^{-3} degree. As shown in Fig. 1(c), the extinction (minimum) angles of $I_{\pm m}$ parabolas is shifted by 0.16 degree, because hydrogenation changes the optical properties of Pd cover layer.[17] Since the MOKE measurement provided the intrinsic magnetic property of H_C and the MO signals, the different responses of H_C and MO signals to hydrogenation will be compared for discussion later in the text.

$$\Delta I = 4\Delta\theta|E_p|^2\phi + constant. \tag{2}$$

Fig. 2 shows the reversibility of the hydrogenation effect. Both the H_C and Kerr intensity were simultaneously recorded in cyclic hydrogenation in 1 atm hydrogen gas. The magnetic coercivity repeatedly increased from 20.4 ± 0.1 Oe to 23.8 ± 0.1 Oe after hydrogenation, and decreased to the original H_C after dehydrogenation by simply pumping out the hydrogen gas from the MOKE chamber and keeping the sample in a vacuum. The magneto-optical Kerr signal was also cyclically enhanced by $17\pm3\%$ after hydrogenation. But
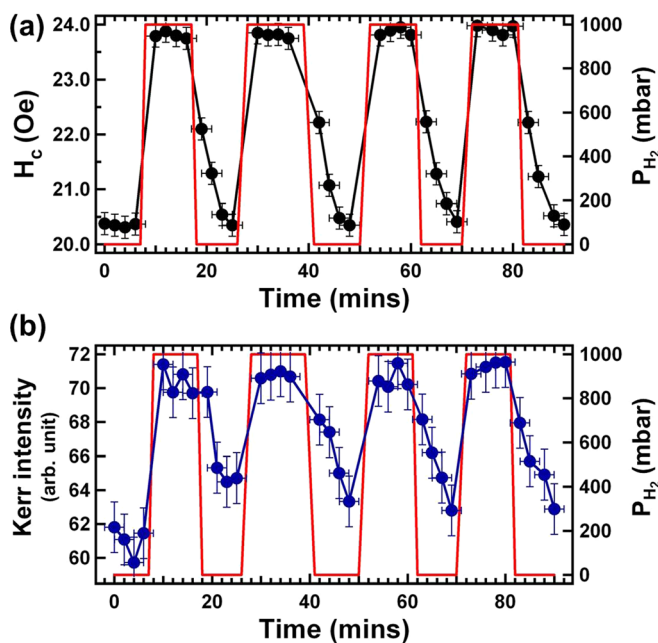

FIG. 2. Reversible variations of (a) magnetic coercivity (H_C) and (b) Kerr intensity (ΔI) with cyclic exposure to 1 atm H$_2$. The red solid lines (right axis) indicate the H$_2$ gas pressure during measurement.

the dehydrogenation did not fully recover the initial value of Kerr intensity, because the 8 min of waiting time after pumping of hydrogen gas is not long enough to recover the initial condition. Our previous studies also reported that the recovering time of MO signals in Pd/Fe, Co, and Ni bilayers actually took 50–200 min, depending on the Pd thickness and surface morphology, since some of the hydrogen atoms in the Pd lattice are hard to desorb.[27,28]

In order to investigate the time constant and the correlation between H_C enhancement and hydrogen gas pressure P_{H_2}, the hydrogenation effect on H_C was monitored as a function of reaction time under the various hydrogen gas pressure from 10 to 1000 mbar. Fig. 3(a) shows the measured H_C as a function of reaction time after hydrogen exposure. For 10 mbar hydrogen, the H_C slowly increased only $\sim$0.2 Oe. After exposure to 30 mbar hydrogen gas for 10 min, the H_C enhancement reached 1.0 Oe. The higher hydrogen gas pressure led to the larger H_C enhancement. When the hydrogen gas pressure reached 400 mbar or even higher up to 1000 mbar, the H_C increased to 23.8 ± 0.1 Oe and the enhancement saturated at $\Delta H_C = 3.4\pm0.1$ Oe. In Fig. 3(a), the solid curves are obtained by fitting the experimental data with a exponential function: $\Delta H_C(t) \propto (1-e^{-t/\tau})$. τ is the time constant of hydrogenation effect on H_C. The fitting curves match the experimental data very well, indicating that the hydrogenation effect of H_C enhancement follows the exponential function. The fitted time constants τ and the measured ΔH_C are plotted in Fig. 3(b) as a function of hydrogen gas pressure. When P_{H_2} is below 100 mbar, the ΔH_C drastically increases with P_{H_2} and the time constant ranges hundreds seconds. While P_{H_2} is above 400 mbar, the hydrogenation effect on H_C completed within 50 s and the ΔH_C saturates at 3.4 ± 0.1 Oe.

In contrast to the quick hydrogen absorption, the hydrogen desorption took a longer time. The magnetic coercivity H_C was recorded as a function of time after pumping out the hydrogen gas from MOKE chamber and keeping the sample in a vacuum of 5×10^{-2} mbar. The time-dependent H_C is plotted in Fig. 3(c) for the samples previously exposed to 10–1000 mbar hydrogen gas. After exposure to 30 mbar hydrogen gas, the recovery of H_C takes $\sim$100 s. For samples exposed to 60–1000 mbar hydrogen gas, the recovery time constant gradually increased to 200–300 s. Besides, as shown in Fig. 3(c), the decay of ΔH_C does not behave like a simple exponential decay. There is always a small kink appearing at $H_C \approx 21.3$ Oe ($\Delta H_C \approx 0.9$ Oe) of the monotonically decreasing curves. At this kink, the slope, $\Delta H_C/\Delta t$, is nearly zero, and afterward the ΔH_C drops down again. Previous studies focus more on the hydrogenation process, including hydrogen dissociation and absorption.[2] Fig. 3(a) shows that when hydrogen gas pressure is above 400 mbar, the hydrogenation effect on H_C saturated within 50 s. However, the dehydrogenation, including hydrogen diffusion toward the surface and then desorption, actually takes a longer time up to hundreds seconds.

We take a closer look on the detailed dehydrogenation processes by simultaneous recording of magneto-optical and magnetic signals. The intrinsic magnetic properties of Pd/Co/Pd trilayers were monitored by continuous measurement of H_C. Besides, the MOKE measurement brings in other two important messages. One is $I_{sum} = I_{+m}+I_{-m}$ and the other one is the Kerr intensity $\Delta I = I_{+m} - I_{-m}$. I_{sum} mainly signifies

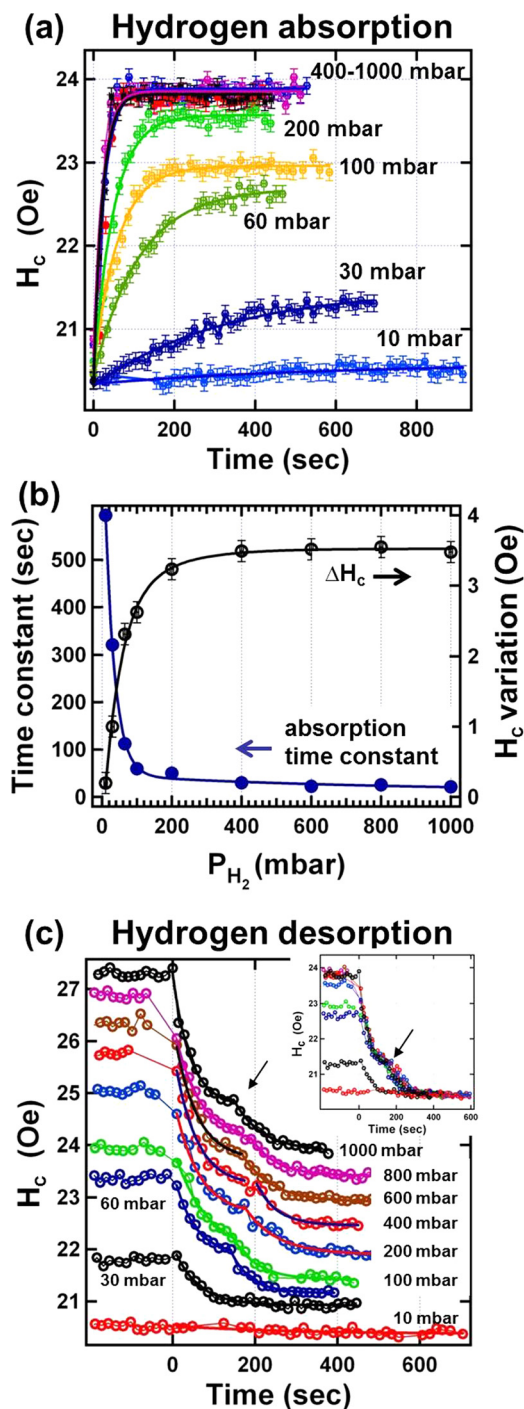## (a) Hydrogen absorption

(b)

(c) Hydrogen desorption

FIG. 3. (a) Time dependent evolution of magnetic coercivity (H_C) after exposure to different H_2 gas pressure. (b) Deduced time constant (left axis) and H_C variation (right axis) plotted as a function of H_2 gas pressure. (c) Time dependent evolution of H_C after pumping out H_2 gas from MOKE chamber. The data curves are vertically shifted for the ease of observation. The inset shows the un-shifted data.

the optical properties of Pd overlayer, while the Kerr intensity ΔI denotes the magneto-optical properties dominated by both the magnetic underlayer and Pd capping layer. The analyzer angle ϕ was set at ~ -2 degree during the MOKE measurement. According to Fig. 1(c), I_{sum} and ΔI increased after hydrogenation. Fig. 4 shows the time dependent measurement of H_C, I_{sum}, and ΔI, while the sample undergoes hydrogenation and then dehydrogenation in sequence. For the ease of comparison, the variations of the three signals are

normalized. After exposure to 200 mbar hydrogen gas, as shown in Fig. 4(a), the I_{sum} value increased and saturated faster than H_C did. This is straightforward because I_{sum} variation is mainly due to the Pd-hydride, while ΔH_C originated from hydrogenation of Pd/Co interface, which is apparently deeper than the Pd capping layer and takes a longer time to achieve. While the hydrogen gas pressure is higher, i.e., 800 mbar as shown in Fig. 4(b), the H_C and I_{sum} increased almost simultaneously. Due to the unstable optical properties and the very small signal, Kerr intensity seriously fluctuated until both the H_C and I_{sum} became stable. Considering the dehydrogenation, right after removing out the hydrogen atmosphere, the I_{sum} significantly dropped down, followed by a moderately decreasing curve. With the higher hydrogen gas exposure, the I_{sum} dropped more seriously at the moment of hydrogen pumping. This indicates that the quick drop of I_{sum} might be due to the fast desorption of β phase hydrogen or the physically absorbed hydrogen on Pd surface. Afterward the α phase hydrogen, which occupied the interstitial sites of the Pd crystalline lattice, gradually desorbed with a relatively slow rate.[2] The microscopic picture of α phase dehydrogenation can be considered as that the hydrogen atoms diffused between the interstitial sites of the crystalline lattice from the underlayer toward the Pd top layer. Therefore, it is intuitive to have first the dehydrogenation of Pd/Co interface and then later the dehydrogenation of Pd cover layer. Fig. 4 shows us the clear experimental result of that H_C decreased
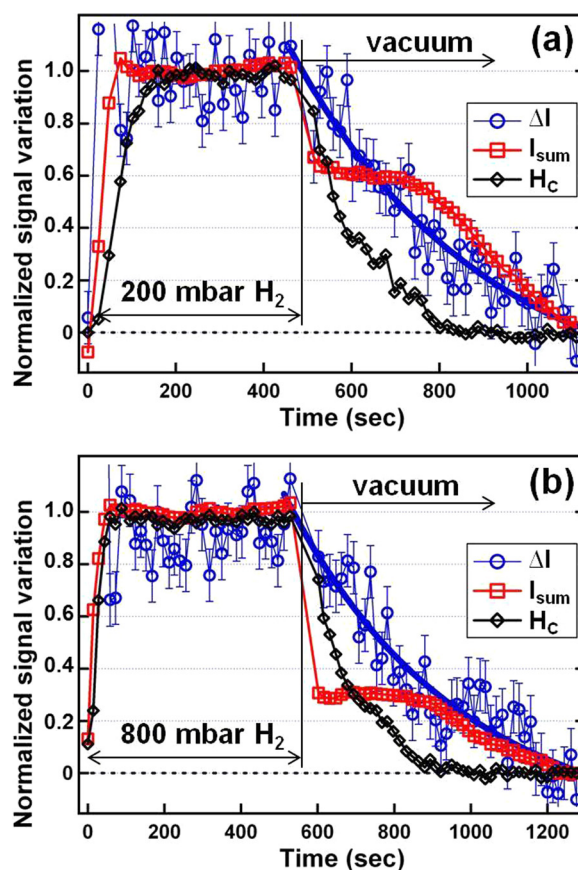

FIG. 4. Time dependent normalized signal variations of H_C, $I_{sum} = I_{+m} + I_{-m}$, and $\Delta I = I_{+m} - I_{-m}$ measured from annealed Pd/Co/Pd/Al$_2$O$_3$(0001). The Pd/Co/Pd sample was exposed to (a) 200 mbar and (b) 800 mbar, respectively, and then dehydrogenated by pumping out H_2 gas. The blue solid lines are the exponential decay fitting to ΔI after dehydrogenation.

and recovers the initial conditions more quickly than I_{sum} did. Since the magneto-optical Kerr intensity originated from the combination of top Pd layer and underline Co layer, the decay speed of ΔI enhancement is in between of H_C and I_{sum}. One noticeable observation is that I_{sum} keeps nearly invariant for a while until H_C recovered the initial value. After the ΔH_C recovery completed, I_{sum} started to decreased again. This coincidence might be because during the desorption of α-phase hydrogen, the diffusion rate of hydrogen atoms from underlayers into Pd top layer equals the desorption rate of hydrogen atoms from Pd surface. There is a period of time, in which the density of hydrogen atoms in Pd top layer is nearly invariant. Until in the Co underlayer the hydrogen is fully removed, the hydrogen density in Pd starts to decrease and thus I_{sum} is reduced again. Besides, the kink appearing during the decay of ΔH_C is coincident with the invariant period of ΔI_{sum}. The appearance of this kink in ΔH_C decay might be another indication of β to α phase transition in the magnetic metal-hydride.

In summary, we demonstrated a reversible modulation of magnetic coercivity H_C in the perpendicularly magnetized Pd/Co/Pd/Al$_2$O$_3$(0001) system by cyclic hydrogenation and dehydrogenation. The H_C enhancement was sensitive to the hydrogen gas pressure P_{H_2} and saturated at $\Delta H_C = 3.4$ Oe when P_{H_2} was above 400 mbar. The response time of H_C enhancement and recovery ranges between tens to hundreds seconds, strongly depending on P_{H_2}. The MO signals reacted faster (slower) than the H_C did after hydrogenation (dehydrogenation). The time-dependent evolution of H_C and MO signals indicates that the significant H_C enhancement originates from the hydrogenation of magnetic layer or interface and provided valuable information for the application of magnetic metal-hydride system.

[1]B. Hjörvarsson, C. Chacon, H. Zabel, and V. Leiner, J. Alloys Compd. **356–357**, 160–168 (2003).

[2]A. Remhof and A. Borgschulte, Chem. Phys. Chem. **9**, 2440 (2008).

[3]Z. Zhao, M. A. Carpenter, H. Xia, and D. Welch, Sens. Actuators B **113**, 532 (2006).

[4]F. J. Ibanñez and F. P. Zamborini, J. Am. Chem. Soc. **130**, 622 (2008).

[5]D. Lederman, Y. Wang, E. H. Morales, R. J. Matelon, G. B. Cabrera, U. G. Volkmann, and A. L. Cabrera, Appl. Phys. Lett. **85**, 615 (2004).

[6]V. K. Valev, M. Di Vece, M. J. Van Beal, D. Grandjean, S. Decoster, A. Vantomme, T. Verbiest, and P. Lievens, J. Appl. Phys. **105**, 114907 (2009).

[7]K. Munbodh, F. A. Perez, C. Keenan, D. Lederman, M. Zhernenkov, and M. R. Fitzsimmons, Phys. Rev. B **83**, 94432 (2011).

[8]M. Suleiman, N. M. Jisrawi, O. Dankert, M. T. Reetz, C. Bähtz, R. Kirchheim, and A. Pundt, J. Alloys Compd. 356–357, **644** (2003).

[9]A. Pundt, M. Suleiman, C. Bähtz, M. T. Reetz, R. Kirchheim, and N. M. Jisrawi, Mater. Sci. Eng. B **108**, 19 (2004).

[10]R. J. Matelon, J. I. Avila, U. G. Volkmann, A. L. Cabrera, E. H. Morales, and D. Lederman, Thin Solid Films **516**, 7797 (2008).

[11]L. Li, F. S. Wen, F. Zhang, Y. F. Lü, Y. F. Lu, Z. Y. Liu, B. Xu, D. L. Yu, J. L. He, and Y. J. Tian, J. Appl. Phys. **107**, 123912 (2010).

[12]F. S. Wen, F. Zhang, Y. F. Lü, J. Y. Xiang, W. Li, Y. F. Lu, Z. Y. Liu, B. Xu, D. L. Yu, J. L. He, and Y. J. Tian, J. Appl. Phys. **110**, 43918 (2011).

[13]B. Hjörvarsson, J. A. Dura, P. Isberg, T. Watanabe, T. J. Udovic, G. Andersson, and C. F. Majkrzak, Phys. Rev. Lett. **79**, 901 (1997).

[14]V. Leiner, K.Westerholt, A. M. Blixt, H. Zabel, and B. Hjörvarsson, Phys. Rev. Lett. **91**, 037202 (2003).

[15]F. Klose, Ch. Rehm, D. Nagengast, H. Maletta, and A. Weidinger, Phys. Rev. Lett. **78**, 1150 (1997).

[16]C. S. Chang, M. Kostylev, and E. Ivanov, Appl. Phys. Lett. **102**, 142405 (2013).

[17]W. C. Lin, C. S. Chi, T. Y. Ho, C. J. Tsai, F. Y. Lo, H. C. Chuang, and M. Y. Chern, J. Appl. Phys. **112**, 063914 (2012).

[18]W. C. Lin, C. S. Chi, T. Y. Ho, and C. J. Tsai, Thin Solid Films **531**, 487 (2013).

[19]D. Weller, H. Brändle, G. Gorman, C.-J. Lin, and H. Notarys, Appl. Phys. Lett. **61**, 2726 (1992).

[20]H. Yamane, Y. Maeno, and M. Kobayashi, J. Appl. Phys. **73**, 334 (1993).

[21]S. Okamoto, O. Kitikami, and Y. Shimada, J. Magn. Magn. Mater. **239**, 313 (2002).

[22]K. Munbodh, F. A. Perez, and D. Lederman, J. Appl. Phys. **111**, 123919 (2012).

[23]K. von Rottkay, M. Rubin, and P. A. Duine, J. Appl. Phys. **85**, 408 (1999).

[24]A. L. Cabrera, J. I. Avila, and D. Lederman, Int. J. Hydrogen Energy **35**, 10613 (2010).

[25]C. P. Romero, J. I. Avila, R. A. Trabol, H. Wang, A. Vantomme, M. J. Van Bael, P. Lievens, and A. L. Cabrera, Int. J. Hydrogen Energy **35**, 2262 (2010).

[26]Z. Q. Qiu and S. D. Bader, Rev. Sci. Instrum. **71**, 1243 (2000).

[27]D. Jose and B. R. Jagirdar, Int. J. Hydrogen Energy **35**, 6804 (2010).

[28]S. Kishore, J. A. Nelson, J. H. Adair, and P. C. Eklund, J. Alloys Compd. **389**, 234 (2005).